Original Article
ln RNA LINC01234 promotes triple-negative breast cancer progression through regulating the miR-429/SYNJ1 axis

Mingyu Bi[1*], Ling Zheng[1*], Li Chen[1], Jixiang He[1], Chao Yuan[1], Ping Ma[1], Yuan Zhao[2], Fei Hu[1], Wenru Tang[1], Miaomiao Sheng[1]

[1]Laboratory of Molecular Genetics of Aging & Tumor, Medical School, Kunming University of Science and Technology, Chenggong Campus, Kunming 650500, Yunnan, China; [2]First People's Hospital of Yunnan Province, Kunming 650032, Yunnan, China. *Equal contributors.

Abstract: Emerging evidence has illustrated that long noncoding RNA 01234 (LINC01234) has played a pivotal role in the development and progression of human cancer. The regulatory role and underlying mechanisms of LINC01234 in triple-negative breast cancer (TNBC) remains unknown. In this study, we analyzed the expression level of LINC01234 in several breast cancer cell lines. CCK-8, EdU, flow cytometry analysis, wound healing assay, and transwell assay were carried out to investigate the effect of LINC01234 on tumor proliferation, apoptosis, and migration. Bioinformatic analysis and luciferase reporter assays were performed to confirm the molecular binding. We found that LINC01234 was dramatically upregulated in breast cancer cell lines, especially in TNBC. The loss and gain-of functional experiments revealed that LINC01234 significantly promoted proliferation, migration, and suppressed cell apoptosis of MDA-MB-231 cells *in vitro* and inhibited tumorigenesis *in vivo.* Mechanistic investigations demonstrated that LINC01234 might act as a competing endogenous RNA (ceRNA) for miR-429 to regulate the SYNJ1 expression. The effects of miR-429 and SYNJ1 in MDA-MB-231 cells were also analyzed. Our results revealed that the novel LINC01234/miR-429/SYNJ1 axis played a critical role in progression of TNBC cell line MDA-MB-231, and it may serve as a therapeutic target for TNBC.

Keywords: LINC01234, miR-429, SYNJ1, triple-negative breast cancer, progression

Introduction

Breast cancer, the most common malignant disease in women, is the second leading cause of cancer-related death [1, 2]. Due to the high heterogeneity of breast cancer, it can be divided into several molecular subtypes. Triple-negative breast cancer (TNBC) is a subtype of breast cancer that does not express estrogen receptor (ER), progesterone receptor (PR), and human epidermal growth factor receptor 2 (HER-2) [3]. It has the characteristics of high invasiveness, high malignancy, and difficult treatment. Due to the primary or secondary drug resistance, or even the lack of specific treatment targets, some patients in the middle- and late-stage lack effective treatments. This is the focus and difficulty in the field of basic research and clinical diagnosis and treatment of breast cancer in the world [4]. It is urgent to

further elucidate the mechanism of the occurrence and development of TNBC at the molecular level, and to find effective diagnostic and prognostic indicators as well as new molecular markers for targeted therapy.

Long-stranded noncoding RNA mainly refers to lncRNA, whose length is between 200-200000 bases. It has the characteristics of low sequence conservation and complex regulatory mechanisms. Studies have reported that LncRNA is involved in many physiological processes, such as gene expression, chromatin remodeling, X-chromosome inactivation, genomic imprinting, RNA splicing, and translation regulation [5, 6]. Its abnormal expression can affect the occurrence and development of many kinds of malignant tumors through a variety of regulatory mechanisms, including breast cancer [7-9]. HOTAIR can promote breast can-

cer metastasis by inducing chromatin rearrangement [10]. lncRNANKILA can inhibit breast cancer metastasis by blocking Iκ-B phosphorylation [11]. Some studies have shown that LncRNA also plays a vital role in TNBC. Shen et al., screened 1758 lncRNAs, and found that the expression of lncRNAXR_250621.1 was significantly higher in clinical samples of TNBC. The expression of lncRNA NONHSAT125629 was significantly lower in TNBC [12]. Eades G studies have found that lncRNA-ROR regulated the progression of TNBC through the lincRNA-RoR-miR-145-ARF6 pathway [13]. These findings suggest that an in-depth study of the biological characteristics of lncRNA and its role in invasion and metastasis are expected to provide a new target for early diagnosis and prognosis monitoring of TNBC.

LINC01234, a newly discovered lncRNA, is located on chromosome 12q24.13. The small number of studies have shown that it was up-regulated in lung cancer [14], gastric cancer [15], and colon cancer [16]. LINC01234 was first reported in breast cancer. Guo et al. found that the three-lncRNA signature (LINC01234 and two other lncRNAs) was an independent prognostic biomarker in breast cancer [17]. The biological function and mechanism of LINC01234, especially in TNBC, remains unknown.

In the present study, we found that LINC01234 was markedly upregulated in TNBC. Loss- and gain-of-function assays showed that LINC01234 promoted TNBC cell line MDA-MB-231 progression *in vitro* and *in vivo*. The mechanistic analysis revealed that LINC01234 functioned as a miR-429 "sponge" and targeted SYNJ1. We demonstrated the important function of LINC01234/miR-429/SYNJ1 axis in TNBC. Our findings may provide a novel therapeutic target for TNBC.

Materials and methods

Cell culture

Four human breast cancer cell lines (MDA-MB-231, MCF-7, T47D, and SK-BR-3) and one non-tumorigenic human breast epithelial cell line (MCF-10A) were purchased from the Peking Union Medical College Cell Culture Center (Beijing, China). They were all cultured in a humidified incubator at 37°C with 5% CO_2. MCF-

10A cells were cultured in DMEM/F12 (12500-062, Thermo Fisher Scientific) medium supplemented with 10% horse serum (HyClone), 1 mg/mL epidermal growth factor (Merck KGaA), 1 mg/mL cholera toxin (Merck KGaA), 20 mg/mL insulin (Merck KGaA), and 1 mg/mL hydrocortisone (Merck KGaA). T47D (Luminal breast cancer cell) and SK-BR-3 cells (HER2-enriched breast cancer cell) were maintained in Roswell Park Memorial Institute-1640 medium (C11875500BT, Thermo Fisher Scientific) supplemented with 10% fetal bovine serum (FBS, 10099141, Thermo Fisher Scientific). MDA-MB-231 (Triple-negative/basal-like breast cancer cell) and MCF-7 cells (Luminal breast cancer cell) were cultured in Dulbecco's modified Eagle's medium (DMEM; C11995500BT, Thermo Fisher Scientific) supplemented with 10% FBS.

Cell transfection

Cells were transfected with small interfering RNAs (siRNAs), plasmid vector, miRNA mimics, miRNA inhibitor, or short hairpin RNA (shRNA) using TransIntro EL transfection reagent (TransGen Biotech, Beijing, China) according to the manufacturer's instructions. The LINC01234 siRNA, SYNJ1 siRNA, miR-429 mimic, miR-429 inhibitor, and matched negative controls were purchased from RiboBio (Guangzhou, China). The pcDNA3.1-LINC01234 plasmid and sh-LINC01234 plasmid were cloned by General Biosystems (Anhui, China).

All the sequences were listed in Supplementary Table 1.

RNA extraction and quantitative RT-PCR assays

We used TRIzol Reagent (T9424, Merck KGaA) to extract the total RNA from tissues and cell lines. Single-stranded complementary DNA was synthesized from RNA using GoScript™ Reverse Transcription System (Promega, Wisconsin, USA) and qRT-PCR analyses were performed using the SYBR Green Master Mix (Roche, Basel, Switzerland). U6 or GAPDH was used as an internal control for miRNA expression or mRNA expression. $2^{-\Delta\Delta ct}$ method was used to calculate the expression level of each gene. ABI 7300 instrument (Life Technology, USA) was used to conduct the qRT-PCR and data collection. The primers were shown in Supplementary Table 1.

Cell proliferation assays

Cell Counting Kit-8 (CCK-8) (RiboBio, Guangzhou, China) was used to detect the cell proliferation. Cells were seeded in 24-well plates, after being transfected with plasmid for 48 h, 50 μL of CCK-8 solution was added to each well. The absorbance was measured at 450 nm using a microplate reader (BioTek) after incubating for 20-40 min at 37°C.

2.5 EdU (5-ethynyl-2'-deoxyuridine) assays

5-ethynyl-2'-deoxyuridine (EdU) was used to assess the growth of breast cancer cells. Cells were seeded in 24-well plates and transfected with plasmid for 48 hours. First, 25 mM of EdU (RiboBio) was added to each well for 2 hours at 37°C. Second, cells were fixed with 4% paraformaldehyde and 0.5% Triton-X. Third, the cells were reacted with Apollo reaction cocktail (RiboBio) for 30 minutes. Hoechst 33342 was used to label cell nuclei. Finally, inverted microscope (TS100, Nikon, Tokyo, Japan) was used to visualize. The percentage of EdU-positive cells was calculated as (EdU-positive cells/Hoechst-stained cells) × 100%.

Flow cytometry analysis

Cells were seeded in 12-well plates and then transfected with si-LINC01234, pcDNA-LINC01234, miRNA mimics, miRNA inhibitor, or si-SYNJ1. After 48 hours, the cells were harvested and stained with 1 μL Annexin V and 2 μL propidium iodide for 30 minutes. They were analyzed by Flow cytometry (Becton Dickinson, Franklin Lakes, USA) according to manufacturer's instructions.

Wound healing assay

Cells were seeded in a 12-well plate and transfected with si-LINC01234, pcDNA-LINC01234, miRNA mimics, miRNA inhibitor, or si-SYNJ1. After 6 hours, the artificial wounds were generated using a pipette tip and the wounded monolayer cells were washed twice with PBS. These cells were cultured for 12 or 24 hours with 1% low serum medium. Olympus microscope (Olympus Corporation, Tokyo, Japan) was used to capture the cell morphology at different times. ImageproPlus6.0 software (Media Cybernetics, USA) was used to analyze the data.

Transwell assays

We used 6.5 mm transwell chambers with 8 μm pores (3422, Corning Incorporated, New York, USA) were used to determine cell migration. Cells were seeded in a 12-well plate and transfected with plasmids. After 48 hours, digested transfected cells were seeded in the upper chamber with 8×10^5 cells and supplemented to 200 μL with the medium of 0.1% FBS, the lower chambers were filled with 500 μL of complete medium. After 24 hours of incubation, the migrated cells on the lower surface of the membrane were fixed with 4% paraformaldehyde in PBS and stained with 0.1% crystal violet. The non-migratory cells that remained in the upper surface were removed with a cotton swab. The cells adhering to the lower chamber were counted with light microscopy.

Luciferase activity analyses

The wild-type (LINC01234-WT) or mutant-type (LINC01234-MUT) fragment and the 3' untranslated region (UTR) of SYNJ1 (SYNJ1-WT or SYNJ1-MUT) were cloned into the PmeI and XbaI sites of the PmirGLO vector (Promega). Both constructs were verified by sequencing. 293T cells were cultured in 12-well plates and were co-transfected with 50 nM control mimic or miR-429 mimic, 2 μg either wild-type vector or mutant vector using Lipofectamine 2000 (Invitrogen). At 48 h post-transfection, the relative luciferase activity was calculated by normalizing the firefly luminescence to the Renilla luminescence using the Dual-Luciferase Reporter Assay (Promega) according to the manufacturer's instructions. Values represent the mean ± standard deviation of three experiments from three independent assays.

Animal experiments

All protocol was approved by the Animal Ethics Committee of the Kunming University of Science and Technology (PZWH K2019-0005). Four-week-old female null mice were purchased from Hunan SJA Laboratory Animal Co., Ltd. 1×10^6 MDA-MB-231 cells that transfected with lentivirus (sh-NC or sh-LINC01234) were injected subcutaneously. Tumor volumes were measured every 7 days. The volume was calculated using the following formula: V=0.5 × length × width^2. After 6 weeks, mice were euthanized, and the tumor weight was examined.

RNA-FISH

MDA-MB-231 cells were inoculated in 48-well plates at a density of 1×10^4 cells/well and cultured overnight in an incubator. Cells were fixed in 4% paraformaldehyde for 20 min and washed with PBS. The fixed cells were treated with proteinase K (20 ug/ml) at 37°C for 8 min and blocked-in pre-hybridization buffer for 1 h. Cells were incubated with probe-containing hybridization solution at 37°C overnight. After cells were washed, they were stained by DAPI for 8 min in the dark. Finally, the slices were observed under a Nikon fluorescence microscope and the images were collected.

RNA immunoprecipitation (RIP)

RIP assays were performed using an EZ-Magna RIP™ RNA-Binding Protein Immunoprecipitation Kit (Millipore, #17-701) according to the manufacturer's protocol. MDA-MB-231 cells (1×10^7) were lysed in complete RIP lysis buffer, remove 100 μL of the supernatant of RIP lysate and incubated with magnetic beads conjugated with anti-Ago2 (Millipore, 03-110) or control IgG for overnight at 4°C. The beads were washed with RIP wash buffer and incubated with proteinase K. The purified RNA was eluted for subsequent qRT-PCR measurement.

Western blot

After transfection, MDA-MB-231 cells were lysed with RIPA lysis buffer (Beyotime Biotechnology, China, P0013B). Protein concentration was measured using BCA Protein Assay Kit (TIANGEN BIOTECH (BEIJING) Co., Ltd. PA115). Cell lysates were separated by 8% SDS-PAGE and transferred to 0.45 μm PVDF membrane (Merck KgaA, IPVH00010), followed by incubation with primary antibodies, including SYNJ1 (Affinity, DF13566, 1:1000), GAPDH (ABclonal, AC001, 1:1000) and Tubulin (ABclonal, AC008, 1:1000) overnight at 4°C. The membranes were washed with Tris-buffered saline and Tween-20 for 10 min and incubated with secondary antibodies for 2 h at room temperature. The protein bands were examined with Immobilon western chemiluminescent reagent (Merck KGaA) and images were captured with a chemiluminescence imaging system (Tanon 5200, Shanghai, China).

Bioinformatics analysis

AnnoLnc database (http://annolnc.cbi.pku.edu.cn/index.jsp) was used to predict the miRNAs of LINC01234 interactions. The targets of candidate miRNAs were predicted using 4 online databases, including TargetScan (http://www.targetscat.org/vert_72/), miRTarBase (http://mirtarbase.mbc.nctu.edu.tw/), miRDB (http://mirdb.org/) and microRNA.org (http://www.microrna.org/microrna/home.do).

Statistical analyses

All statistical analyses were performed by SPSS version 19 software (IBM Corp., Armonk, USA) and GraphPad Prism 7 (GraphPad Software, La Jolla, USA). Data were shown as the mean ± standard deviation (SD). Statistical differences were determined by using the students' t test or ANOVA analysis. $P<0.05$ was defined as statistically significant.

Results

LINC01234 was upregulated in TNBC

To study the role of LINC01234 in breast cancer, we first detected the LINC01234 levels in breast cancer cell lines and non-tumorigenic mammary epithelial cell line (MCF-10A). As shown in the Supplementary Figure 1, LINC01234 was up-regulated in all four breast cancer cell lines compared with the MCF-10A. The highest expression was found in TNBC cell line (MDA-MB-231), suggesting that LINC01234 may promote the progression of TNBC.

Knockdown of LINC01234 inhibited TNBC cells proliferation and cell migration but induces cell apoptosis

To investigate the biological function of LINC01234 in TNBC cells, we first knocked down or overexpressed LINC01234 in MDA-MB-231 cells. The transfection efficiency was confirmed by qRT-PCR (**Figure 1A** and **1B**). CCK-8 assays demonstrated that silencing of LINC01234 significantly inhibited the proliferation of MDA-MB-231 cells. LINC01234 overexpression significantly increased cell growth (**Figure 1C** and **1D**). EdU assays revealed that knockdown of LINC01234 markedly decreased the percentages of EdU-positive cells. The opposite effects were observed after LINC01234 overexpression (**Figure 1E** and **1F**).
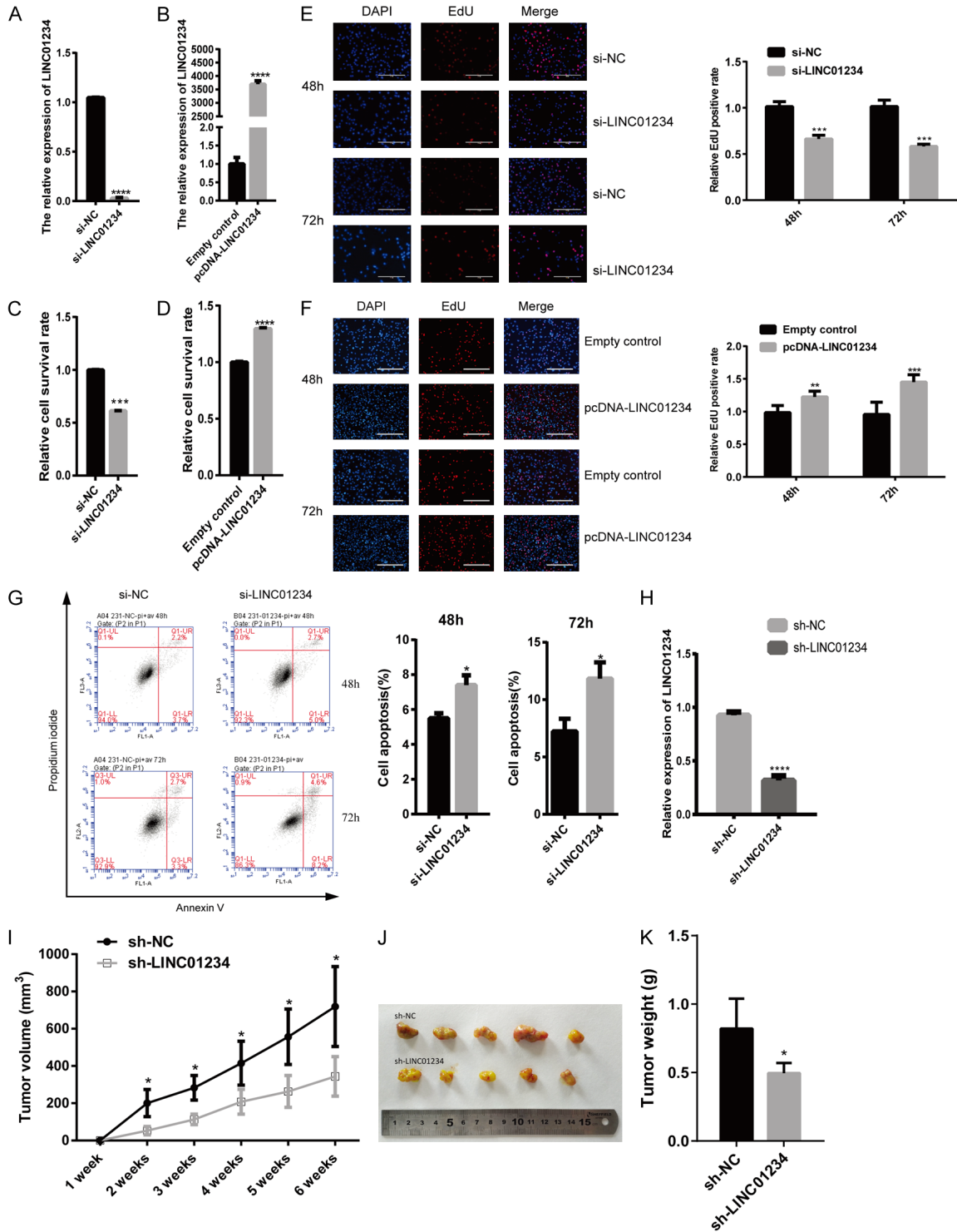
Figure 1. Knockdown of LINC01234 inhibited TNBC cell proliferation and induces cell apoptosis *in vitro* and *in vivo*. A. qRT-PCR analysis of LINC01234 expression in MDA-MB-231 cells transfected with si-NC or si-LINC01234. B. qRT-PCR analysis of LINC01234 expression in MDA-MB-231 cells transfected with empty control or pcDNA-LINC01234. C and D. The effect of LINC01234 on cell proliferation was evaluated by CCK-8 assays. E and F. EdU assays assessed the effect of LINC01234 on cell proliferation. Scale bar: 200 μm (100 ×). G. FACS was performed to determine the apoptosis rate. H. qRT-PCR analysis of LINC01234 expression in MDA-MB-231 cells transfected with sh-RNA. I. Tumor volumes were measured once a week (N=5). J. Images of tumors of each group. K. Tumor weights were evaluated at the end of experiment. NC, negative control. EdU, 5-Ethynyl-2'-deoxyuridine. FACS, fluorescence activated cell sorting. The data were representative of 3 independent experiments with the mean ± standard deviation. *$P<0.05$, **$P<0.01$, ***$P<0.001$, ****$P<0.0001$.
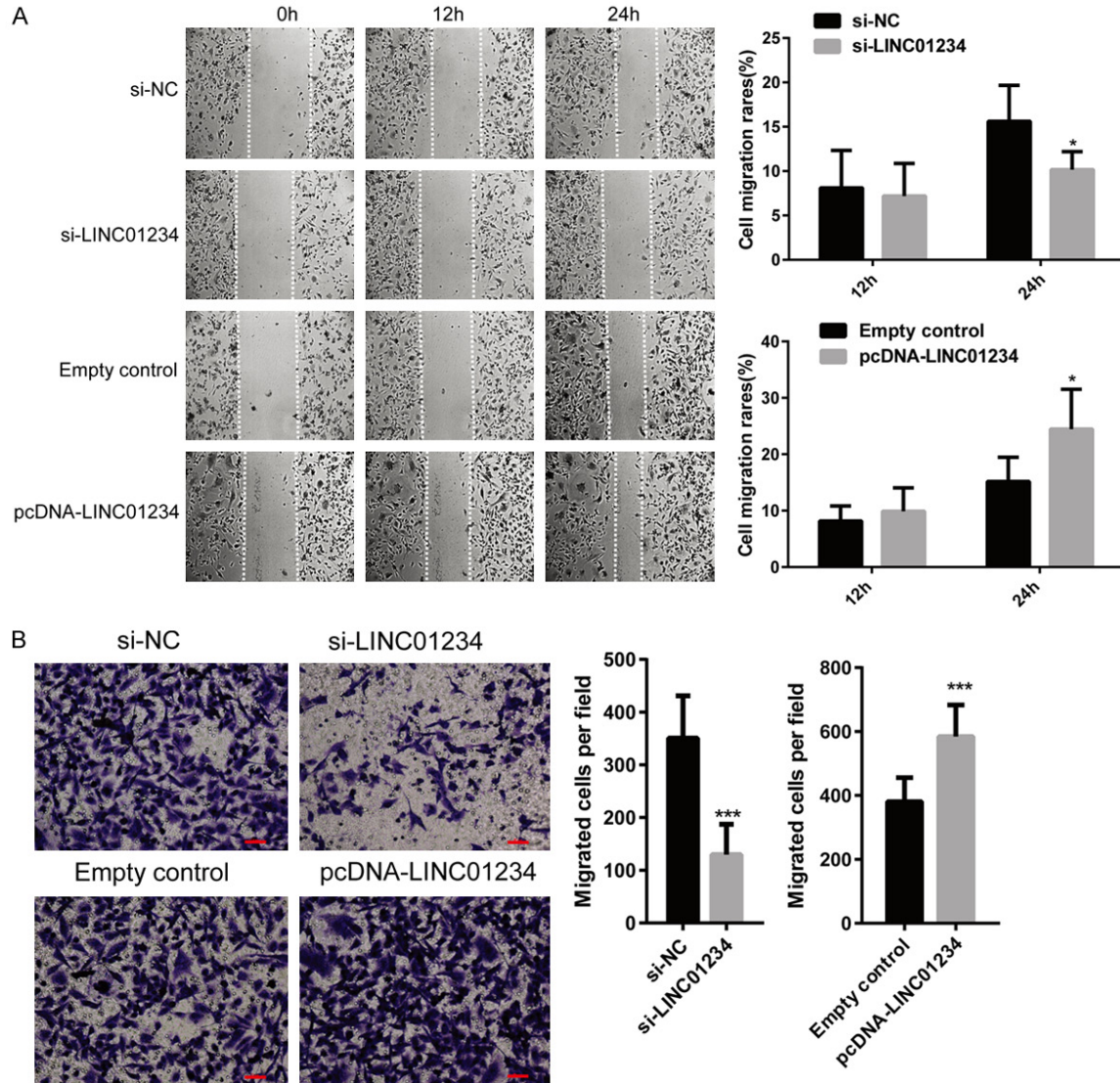
Figure 2. LINC01234 promoted TNBC cell migration. The migration capacity of MDA-MB-231 cell transfected with indicated vectors was detected by wound-healing assay (A) and transwell assay (B) Scale bar: 50 μm (200 ×). NC, negative control. The data were representative of 3 independent experiments with the mean ± standard deviation. $^*P<0.05$, $^{***}P<0.001$.

We explored the effect of LINC01234 on apoptosis of MDA-MB-231 cells. Flow cytometry analysis showed that the apoptotic ratio of MDA-MB-231 cells was significantly increased by knocking down LINC01234 (**Figure 1G**).

The xenograft assay was carried out to explore whether LINC01234 affected the tumor growth *in vivo*. MDA-MB-231 cells were stably transfected with sh-LINC01234 or control vector and then subcutaneously injected into female nude mice. The transfection efficiency was confirmed by qRT-PCR (**Figure 1H**). Consistent with the *in vitro* results, the tumor volume and tumor weight were significantly reduced in sh-LINC01234 group compared with sh-control group (**Figure 1I-K**).

These data suggested that LINC01234 promoted the progression of MDA-MB-231 cells *in vitro* and *in vivo*.

We evaluated the effect of LINC01234 on cell migration. Wound healing assay indicated that knockdown of LINC01234 in MDA-MB-231 cells remarkably decreased the cell migration.
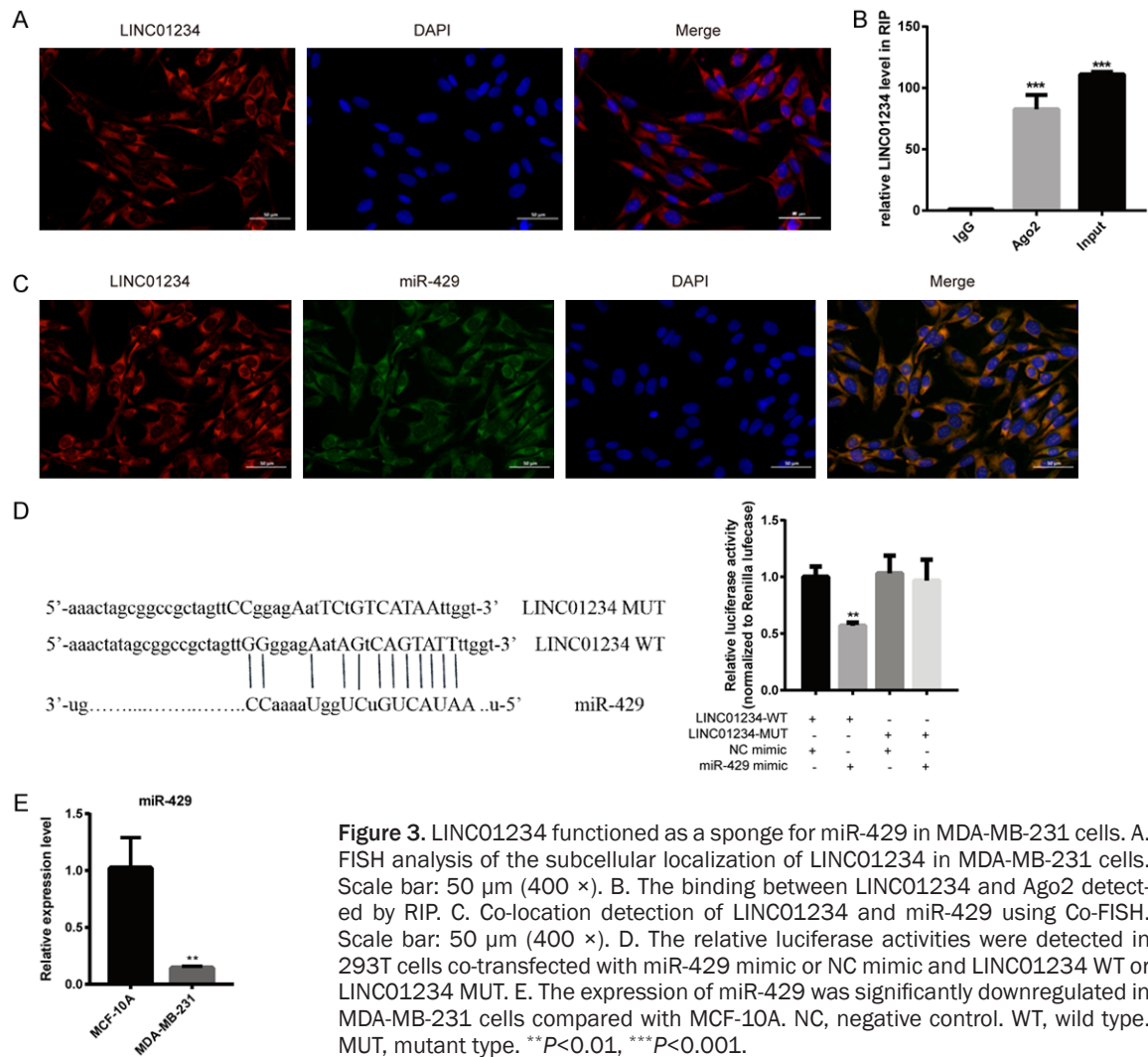
Figure 3. LINC01234 functioned as a sponge for miR-429 in MDA-MB-231 cells. A. FISH analysis of the subcellular localization of LINC01234 in MDA-MB-231 cells. Scale bar: 50 μm (400 ×). B. The binding between LINC01234 and Ago2 detected by RIP. C. Co-location detection of LINC01234 and miR-429 using Co-FISH. Scale bar: 50 μm (400 ×). D. The relative luciferase activities were detected in 293T cells co-transfected with miR-429 mimic or NC mimic and LINC01234 WT or LINC01234 MUT. E. The expression of miR-429 was significantly downregulated in MDA-MB-231 cells compared with MCF-10A. NC, negative control. WT, wild type. MUT, mutant type. $^{**}P<0.01$, $^{***}P<0.001$.

Overexpression of LINC01234 significantly promoted the migration of treated cells (**Figure 2A**). The same results were obtained using wound assays. The number of migrated MDA-MB-231 cells were dramatically suppressed by LINC01234 knockdown, but significantly enhanced by upregulated of LINC01234 (**Figure 2B**). These data indicated that LINC01234 contributed to TNBC cells migration.

LINC01234 functioned as a sponge for miR-429 in MDA-MB-231 cells

To better understand the molecular mechanism of LINC01234, we examined its distribution by FISH. The result showed that LINC01234 was more located in the cytoplasm (**Figure 3A**). RIP experiment was performed. It indicated that LINC01234 could directly bind to Ago2 (a component of the RNA induced silencing complex) (**Figure 3B**). This finding suggested that LINC01234 could be used as a ceRNA to play its regulatory function.

To verify this hypothesis, we used the AnnoLnc online database to predict the miRNAs that may be regulated by LINC01234. The results showed that LINC01234 might contain nine miRNAs binding sites. To identify the specific target miRNA of LINC01234, we detected the expression of these miRNAs by knockdown or overexpression of LINC01234. We found that silencing of LINC01234 could significantly increase the level of miR-429. Overexpression of LINC01234 could markedly decrease the expression of miR-429 (Supplementary Figure 2A and 2B). Co-FISH analysis showed that LINC01234 and miR429 were co-located
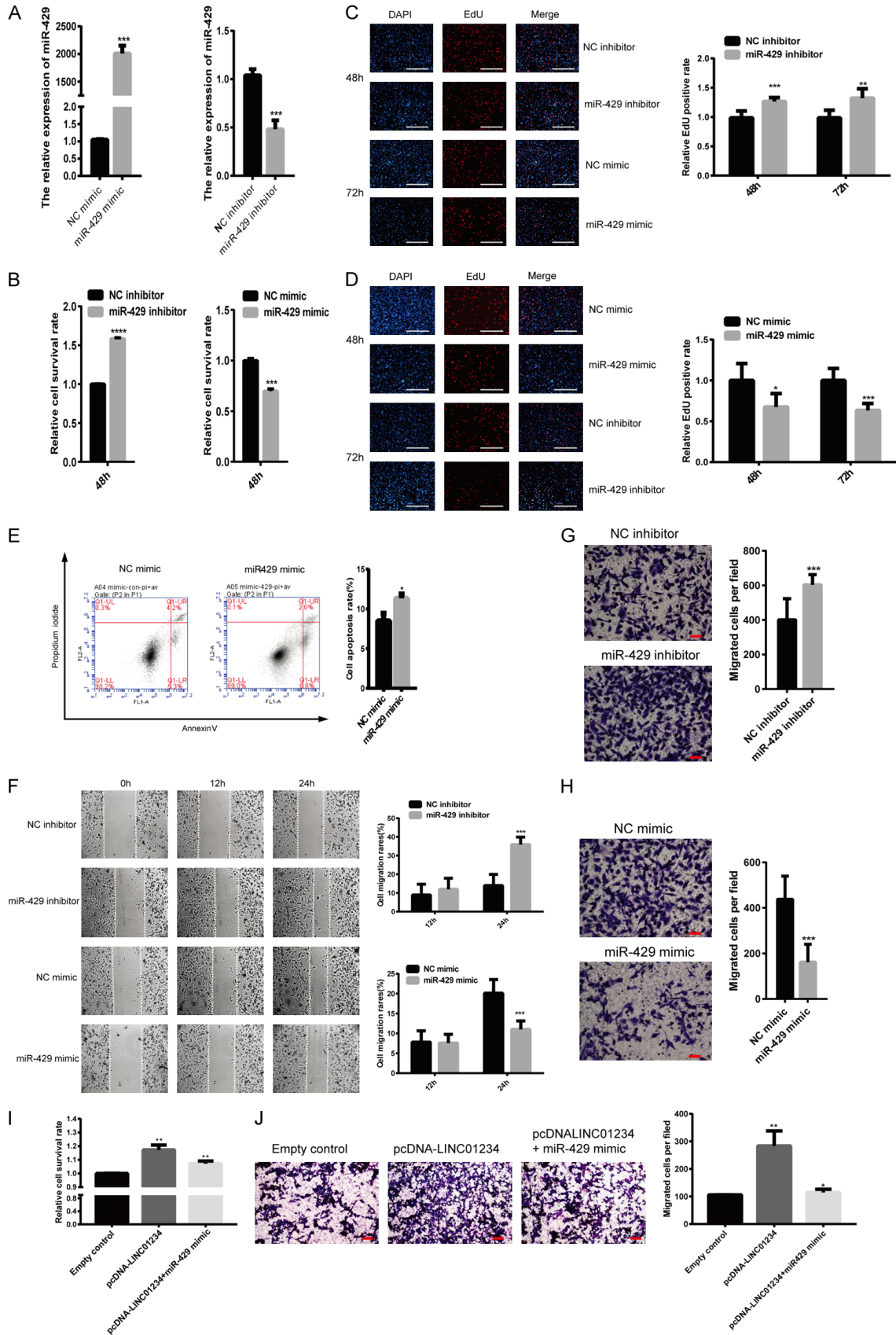
Figure 4. Effect of miR-429 on TNBC cells proliferation, apoptosis, and migration. (A) qRT-PCR analysis of miR-429 expression in MDA-MB-231 cells transfected with miR-429 mimic or miR-429 inhibitor. (B) The effect of miR-429 on cell proliferation was evaluated by CCK-8 assays. (C and D) EdU assays assessed proliferation of MDA-MB-231 cells transfected with miR-429 inhibitor or miR-429 mimic. Scale bar: 200 μm (100 ×). (E) The influence of miR-429 mimic on cell apoptosis was evaluated by flow cytometry. Cell migration was determined after infection with miR-429 inhibitor or miR-429 mimic using wound-healing assay (F) and transwell assay (G and H) Scale bar: 50 μm (200 ×). (I) CCK-8 assays were performed to analysis cell proliferation when MDA-MB-231 cells co-transfected with pcDNA-LINC01234, miR-429 or empty control. (J) Transwell assays of MDA-MB-231 cells co-transfected with pcDNA-LINC01234, miR-429 mimic, or empty control. Scale bar: 100 μm (100 ×). NC, negative control. EdU, 5-Ethynyl-2'-deoxyuridine. $^*P<0.05$, $^{**}P<0.01$, $^{***}P<0.001$, $^{****}P<0.0001$.

(**Figure 3C**). Dual-luciferase reporter assay was used to verify the association between miR-429 and LINC01234. Results showed that miR-429 mimic could significantly reduce the luciferase activity of wild-type LINC01234, but not the mutant group (**Figure 3D**), suggesting that miR-429 could bind directly to LINC01234. The expression of miR-429 was significantly down-regulated in MDA-MB-231 cells (**Figure 3E**). We chose miR-429 as a candidate gene for further study.

Effect of miR-429 on TNBC cells proliferation, apoptosis, and migration

In exploring the roles of miR-429 in TNBC cells, we transfected miR-429 mimic and inhibitor into MDA-MB-231 cells. The transfection efficiency is shown in **Figure 4A**. CCK-8 and EdU assays showed that silencing of miR-429 promoted cell proliferation, and overexpression of miR-429 inhibited cell proliferation (**Figure 4B-D**). Flow cytometry analysis revealed that miR-429 mimics could induce cell apoptosis (**Figure 4E**). We evaluated whether miR-429 affected MDA-MB-231 cells migration. Wound healing and transwell assays indicated that miR-429 inhibitor increased the migration capabilities of MDA-MB-231 cells. miR-429 mimic produced the opposite effect (**Figure 4F-H**). To determine whether miR-429 was involved in mediating the effects of LINC0-1234 in MDA-MB-231 cells, we co-transfected LINC01234 and miR-429. The results showed that miR-429 mimic partially reversed the cell proliferation and migration induced by LINC01234 overexpression (**Figure 4I-J**).

Effect of SYNJ1 on TNBC cells proliferation, apoptosis, and migration

We used miRTarBase, miRDB, microRNA.org, and TargetScan databases to predict the target genes of miR-429. We preliminarily screened 15 candidate target genes. We selected SYNJ1 as the downstream target gene of miR-429,

which confirmed qRT-PCR (Supplementary Figure 3A and 3B). Western blot analysis indicated that SYNJ1 protein levels was increased in respond to miR-429 inhibitor (Supplementary Figure 3C). To validate the direct interaction between miR-429 and SYNJ1, we constructed two luciferase reporter vectors containing the wild-type or mutant SYNJ1 3'UTR. Results showed that the luciferase activity was significantly lower in 293T cells co-transfected with SYNJ1-WT. miR-429 mimic compared with control groups (**Figure 5A**), suggesting that miR-429 was able to bind with the 3'UTR of SYNJ1 directly. As described above, LINC01234 can sponge miR-429. We verified whether LINC01234 could regulate the expression of SYNJ1 in TNBC cells. We found that the SYNJ1 mRNA level and protein level was markedly decreased or increased by knockdown or over-expression of LINC01234 in MDA-MB-231 cells (**Figure 5B**, **5C** and Supplementary Figure 3D). A decrease of SYNJ1 caused by si-LINC01234 was partly reversed by miR-429 inhibitor (**Figrue 5D**). Collectively, LINC01234 could regulate the level of SYNJ1 through modulating miR-429.

To verify the role of SYNJ1 in TNBC, we first detected the expression of SYNJ1 in MDA-MB-231 cells. Results showed that the SYNJ1 was increased in MDA-MB-231 cells compared with MCF-10A (Supplementary Figure 3E). Then, MDA-MB-231 cells were transfected with SYNJ1 siRNA, the silencing efficiency was shown in **Figure 5E**. Knockdown of SYNJ1 significantly reduced the proliferation of MDA-MB-231cells (**Figure 5F**) and increased cell apoptosis (**Figure 5G**). The ability of cell migration was dramatically decreased after transfection with SYNJ1 siRNA (**Figure 5H** and **5I**).

Discussion

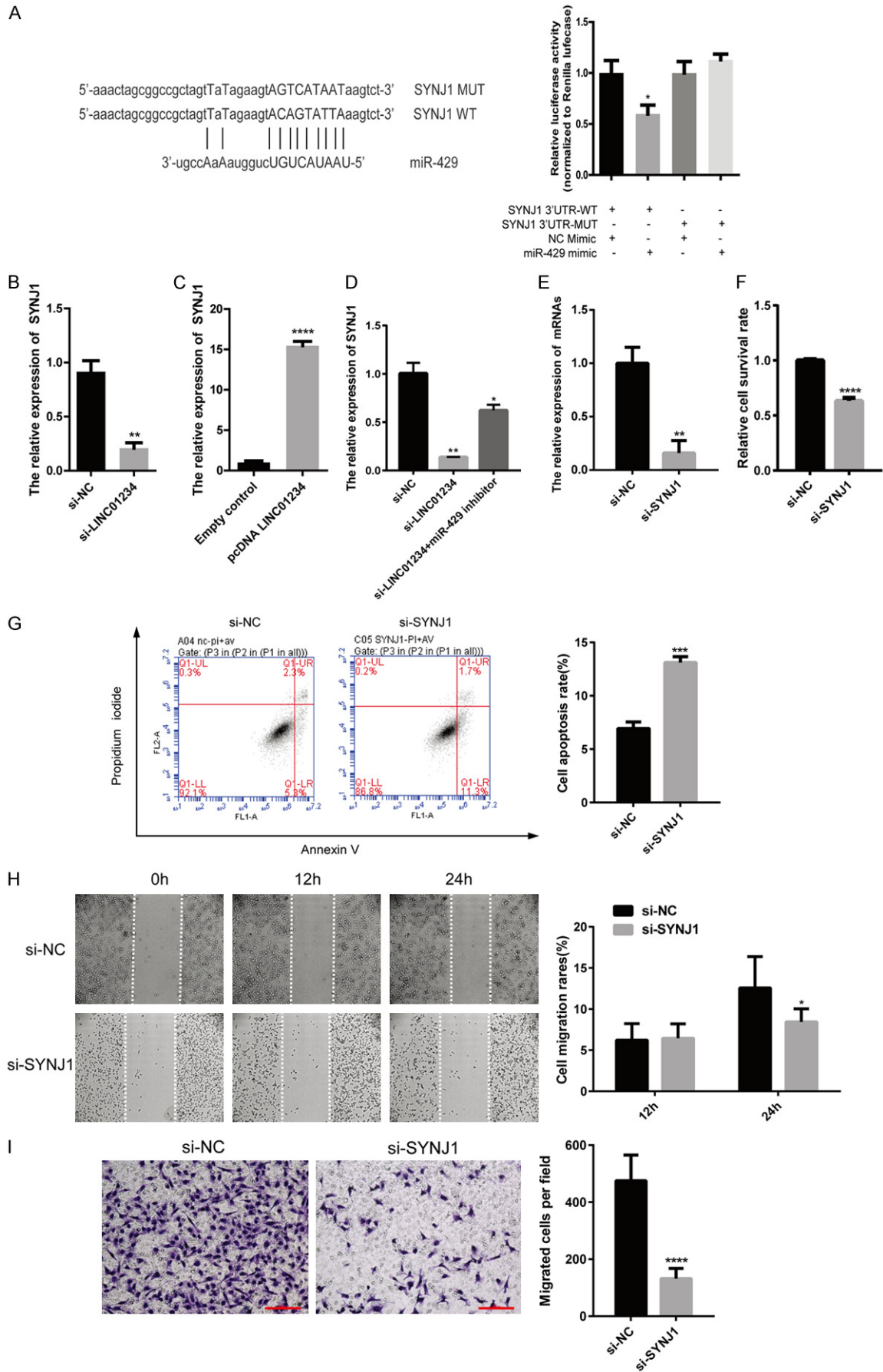Breast cancer is the most common malignant tumor in women all over the world. With the in-

Figure 5. Effects of SYNJ1 on TNBC cells proliferation, apoptosis, and migration. (A) The relative luciferase activities were detected in 293T cells co-transfected with miR-429 mimic or NC mimic and SYNJ1 WT or SYNJ1 MUT. The expression level of SYNJ1 in MDA-MB-231 following knockdown (B) or overexpression (C) of LINCO1234. (D) qRT-PCR analysis of SYNJ1 expression after co-transfection with si-LINCO1234 and miR-429 inhibitor. (E) qRT-PCR analysis of SYNJ1 expression in MDA-MB-231 cells transfected with SYNJ1 siRNA. (F) The effect of SYNJ1 on cell proliferation was evaluated by CCK-8 assays. (G) The influence of SYNJ1 knockdown on cell apoptosis was evaluated by flow cytometry. Cell migration was determined after infection with SYNJ1 siRNA using wound-healing assay (H) and transwell assay (I) Scale bar: 100 µm (200 ×). NC, negative control. EdU, 5-Ethynyl-2'-deoxyuridine. WT, wild type. MUT, mutant type. $^*P<0.05$, $^{**}P<0.01$, $^{***}P<0.001$, $^{****}P<0.0001$.

depth study of breast cancer, it has been found that breast cancer is a type of heterogeneous disease. There are significant differences in clinicopathology and prognosis among different molecular types [18]. TNBC often occurs in young women. The incidence of breast cancer patients is about 10%-20%. Compared with other types of breast cancer, TNBC has the characteristics of high histopathological grade, high degree of invasiveness, short survival time, and poor prognosis [19]. Some studies have shown that the median survival time of patients with invasive TNBC was only 13 months. Systemic therapy based on chemotherapy was not effective for such patients [20]. The key to improve the prognosis of TNBC is to clarify the mechanism of occurrence and development of TNBC at the molecular level and to identify effective biological treatment targets.

The discovery of long noncoding RNA has changed our understanding of transcriptional and post-transcriptional regulation. With the development of high-throughput sequencing and other new technologies, LncRNAs have become the focus of cancer research. It can regulate gene expression and cell biological function through a variety of mechanisms [21]. At present, dozens of LncRNAs, related to breast cancer, such as HOTAIR [10, 22], GAS5 [23], MALAT [24], and H19 [25] have been identified. They can affect the occurrence and development of breast cancer by regulating epigenetic modification and key cellular signal transduction.

In this article, we focused on LINCO1234. Guo et al. revealed that LINCO1234 combined with the other two LncRNAs can be used as prognostic markers of breast cancer [17]. The role of LINCO1234 in NSCLC [14], colon cancer [16], gastric cancer [15], and liver cancer [26] has been reported. The molecular mechanism of LINCO1234 in TNBC has not been reported. We

found that compared with MCF-10A, LINCO-1234 was highly expressed in MDA-MB-231, MCF-7, T47D, and SK-BR-3 cells, especially in TNBC cell line. MDA-MB-231, which predicted that LINCO1234 might contribute to the development of TNBC. We carried out loss- and gain-of-function assays to explore whether LINCO1234 can influence the process of MDA-MB-231 cells. *In vitro* and *in vivo* experiments showed that knockdown of LINCO1234 significantly inhibited cell proliferation and migration, and induced cell apoptosis. Overexpression of LINCO1234 significantly promoted the cell proliferation and migration, and suppressed cell apoptosis, suggesting that LINCO1234 may play an important oncogenic role in TNBC tumorigenesis.

The regulation of LncRNA on miRNA is an important part of its function. Studies have shown that LncRNA can regulate gene expression by competitively binding with miRNA. For example, lncRNAZFAS1 can be used as miR-150 sponge to regulate the expression of ZEB1, MMP14, and MMP16, thus promoting the metastasis of hepatocellular carcinoma [27]. To identify the underlying molecular mechanism of LINC-01234, we used bioinformatics, analyses, and luciferase reporter assays and found that LINCO1234 could directly sponge miR-429. MiR-429 is a member of the miR-200 family. Researches have shown that miR-429 disorders are related to the occurrence, development, invasion, and metastasis of many kinds of cancers [28-30]. In different tumor types, miR-429 can play a role as tumor suppressor gene or tumor promoting gene respectively [31]. We found that miR-429 was significantly downregulated in MDA-MB-231 cells. Overexpression of miR-429 significantly impaired cell proliferation and migration, and induced cell apoptosis, which was consistent with previous reports [32, 33]. We found that the cell proliferation and migration induced by LINCO1234 overexpression could be reversed by miR-429

mimic. These data indicated that LINC01234 exerted oncogenic effects through regulating miR-429.

In general, miRNA mediates the binding of the silencing complex RISC to the 3'UTR of the target gene, leading to degradation or translation inhibition of the target gene. We identified a new target gene of miR-429, SYNJ1, through online predicting database and luciferase reporter assays. These reports of SYNJ1 are extremely rare. In 2014, SYNJ1 mutation was found in Parkinson's disease [34]. Then, in 2015, it was reported that SYNJ1 was a 5'phosphatase, which can regulate vesicle recirculation and availability of nerve endings, and found that SYNJ1 was a homologue of SYNJ2, an effector of Rho family GTP enzyme Rac1. Studies showed that SYNJ2 was highly overexpressed in many invasive breast cancer patients' tumors. Knockout of SYNJ2 can inhibit the growth and lung metastasis of breast tumors in mice, indicating that SYNJ2 was a drug target to block the migration of cancer cells [35]. The role of SYNJ1 in TNBC has not been reported yet. In the present study, we found that SYNJ1 was upregulated in MDA-MB-231 cells, and we first revealed that knockdown of SYNJ1 can inhibit MDA-MB-231 cell proliferation, migration, and promote cell apoptosis. At the same time, knockdown, or overexpression of LINC01234 can decrease or increase the expression of SYNJ1, suggesting that LINC01234 could regulate SYNJ1 function through inhibiting miR-429.

There are several limitations in this study. First, we need to collect clinical samples, especially the samples of patients with TNBC, to clarify the correlation between LINC01234 and clinicopathological indexes and prognosis of TNBC patients. Secondly, we only carried out the *in vivo* experiment of LINC01234. The roles of miR-429 and SYNJ1 *in vivo* were also needed to confirm. The precise molecular mechanism of LINC01234 on SYNJ1 was required to investigated. Third, the function of LINC01234 in other types of breast cancer remained to be studied.

In summary, we studied the mechanism of LINC01234 on TNBC for the first time and revealed that LINC01234 can be used as ceRNA to regulate the expression of SYNJ1 by sponging miR-429. Based on our data, LINC01234/miR-429/SYNJ1 may be used as a novel therapeutic target for patients with TNBC.

Acknowledgements

Disclosure of conflict of interest

None.

Address correspondence to: Drs. Miaomiao Sheng and Wenru Tang, Laboratory of Molecular Genetics of Aging & Tumor, Medical School, Kunming University of Science and Technology, Chenggong Campus, 727 South Jingming Road, Kunming 650500, Yunnan, China. Tel: +86-871-65920753; E-mail: shengmm@kust.edu.cn (MMS); twr@sina.com (WRT)

References

[1] Schneider AP, Zainer CM, Mullen NK and Windisch AK. The breast cancer epidemic: 10 facts. Linacre Q 2014; 81: 244-277.

[2] Fan L, Strasser-Weippl K, Li JJ, St Louis J, Finkelstein DM, Yu KD, Chen WQ, Shao ZM and Goss PE. Breast cancer in China. Lancet Oncol 2014; 15: e279-289.

[3] Coates AS, Winer EP, Goldhirsch A, Gelber RD, Gnant M, Piccart-Gebhart M, Thurlimann B and Senn HJ; Panel Members. Tailoring therapies--improving the management of early breast cancer: St Gallen international expert consensus on the primary therapy of early breast cancer 2015. Ann Oncol 2015; 26: 1533-1546.

[4] Garcia-Closas M, Gunsoy NB and Chatterjee N. Combined associations of genetic and environmental risk factors: implications for prevention of breast cancer. J Natl Cancer Inst 2014; 106: dju305.

[5] Lin C and Yang L. Long noncoding RNA in cancer: wiring signaling circuitry. Trends Cell Biol 2018; 28: 287-301.

[6] Kopp F and Mendell JT. Functional classification and experimental dissection of long noncoding RNAs. Cell 2018; 172: 393-407.

[7] Pang B, Wang Q, Ning S, Wu J, Zhang X, Chen Y and Xu S. Landscape of tumor suppressor long noncoding RNAs in breast cancer. J Exp Clin Cancer Res 2019; 38: 79.

[8] Wang G, Liu C, Deng S, Zhao Q, Li T, Qiao S, Shen L, Zhang Y, Lu J, Meng L, Liang C and Yu

Z. Long noncoding RNAs in regulation of human breast cancer. Brief Funct Genomics 2016; 15: 222-226.

[9] Soudyab M, Iranpour M and Ghafouri-Fard S. The role of long non-coding RNAs in breast cancer. Arch Iran Med 2016; 19: 508-517.

[10] Gupta RA, Shah N, Wang KC, Kim J, Horlings HM, Wong DJ, Tsai MC, Hung T, Argani P, Rinn JL, Wang Y, Brzoska P, Kong B, Li R, West RB, van de Vijver MJ, Sukumar S and Chang HY. Long non-coding RNA HOTAIR reprograms chromatin state to promote cancer metastasis. Nature 2010; 464: 1071-1076.

[11] Liu B, Sun L, Liu Q, Gong C, Yao Y, Lv X, Lin L, Yao H, Su F, Li D, Zeng M and Song E. A cytoplasmic NF-kappaB interacting long noncoding RNA blocks IkappaB phosphorylation and suppresses breast cancer metastasis. Cancer Cell 2015; 27: 370-381.

[12] Shen X, Xie B, Ma Z, Yu W, Wang W, Xu D, Yan X, Chen B, Yu L, Li J, Chen X, Ding K and Cao F. Identification of novel long non-coding RNAs in triple-negative breast cancer. Oncotarget 2015; 6: 21730-21739.

[13] Eades G, Wolfson B, Zhang Y, Li Q, Yao Y and Zhou Q. lincRNA-RoR and miR-145 regulate invasion in triple-negative breast cancer via targeting ARF6. Mol Cancer Res 2015; 13: 330-338.

[14] Xie JJ, Guo QY, Jin JY and Jin D. SP1-mediated overexpression of lncRNA LINC01234 as a ceRNA facilitates non-small-cell lung cancer progression via regulating OTUB1. J Cell Physiol 2019; 234: 22845-22856.

[15] Chen X, Chen Z, Yu S, Nie F, Yan S, Ma P, Chen Q, Wei C, Fu H, Xu T, Ren S, Sun M and Wang Z. Long noncoding RNA LINC01234 functions as a competing endogenous RNA to regulate CBFB expression by sponging miR-204-5p in gastric cancer. Clin Cancer Res 2018; 24: 2002-2014.

[16] Lin C, Zhang Y, Chen Y, Bai Y and Zhang Y. Long noncoding RNA LINC01234 promotes serine hydroxymethyltransferase 2 expression and proliferation by competitively binding miR-642a-5p in colon cancer. Cell Death Dis 2019; 10: 137.

[17] Guo W, Wang Q, Zhan Y, Chen X, Yu Q, Zhang J, Wang Y, Xu XJ and Zhu L. Transcriptome sequencing uncovers a three-long noncoding RNA signature in predicting breast cancer survival. Sci Rep 2016; 6: 27931.

[18] Yeo SK and Guan JL. Breast cancer: multiple subtypes within a tumor? Trends Cancer 2017; 3: 753-760.

[19] Papa A, Caruso D, Tomao S, Rossi L, Zaccarelli E and Tomao F. Triple-negative breast cancer: investigating potential molecular therapeutic target. Expert Opin Ther Targets 2015; 19: 55-75.

[20] Denkert C, Liedtke C, Tutt A and von Minckwitz G. Molecular alterations in triple-negative breast cancer-the road to new treatment strategies. Lancet 2017; 389: 2430-2442.

[21] Wilusz JE, Sunwoo H and Spector DL. Long noncoding RNAs: functional surprises from the RNA world. Genes Dev 2009; 23: 1494-1504.

[22] Padua Alves C, Fonseca AS, Muys BR, de Barros E Lima Bueno R, Burger MC, de Souza JE, Valente V, Zago MA and Silva WA Jr. Brief report: the lincRNA Hotair is required for epithelial-to-mesenchymal transition and stemness maintenance of cancer cell lines. Stem Cells 2013; 31: 2827-2832.

[23] Pickard MR and Williams GT. The hormone response element mimic sequence of GAS5 lncRNA is sufficient to induce apoptosis in breast cancer cells. Oncotarget 2016; 7: 10104-10116.

[24] Zhao Z, Chen C, Liu Y and Wu C. 17beta-Estradiol treatment inhibits breast cell proliferation, migration and invasion by decreasing MALAT-1 RNA level. Biochem Biophys Res Commun 2014; 445: 388-393.

[25] Li Z, Li Y, Li Y, Ren K, Li X, Han X and Wang J. Long non-coding RNA H19 promotes the proliferation and invasion of breast cancer through upregulating DNMT1 expression by sponging miR-152. J Biochem Mol Toxicol 2017; 31.

[26] Chen Y, Zhao H, Li H, Feng X, Tang H, Zhang J, Fu B and Qiu C. LINC01234/MicroRNA-31-5p/MAGEA3 axis mediates the proliferation and chemoresistance of hepatocellular carcinoma cells. Mol Ther Nucleic Acids 2019; 19: 168-178.

[27] Li T, Xie J, Shen C, Cheng D, Shi Y, Wu Z, Deng X, Chen H, Shen B, Peng C, Li H, Zhan Q and Zhu Z. Amplification of long noncoding RNA ZFAS1 promotes metastasis in hepatocellular carcinoma. Cancer Res 2015; 75: 3181-3191.

[28] Kong X, Ding X, Li X, Gao S and Yang Q. 53BP1 suppresses epithelial-mesenchymal transition by downregulating ZEB1 through microRNA-200b/429 in breast cancer. Cancer Sci 2015; 106: 982-989.

[29] Wu G, Zheng H, Xu J, Guo Y, Zheng G, Ma C, Hao S, Liu X, Chen H, Wei S, Song X and Wang X. miR-429 suppresses cell growth and induces apoptosis of human thyroid cancer cell by targeting ZEB1. Artif Cells Nanomed Biotechnol 2019; 47: 548-554.

[30] Fan JY, Fan YJ, Wang XL, Xie H, Gao HJ, Zhang Y, Liu M and Tang H. miR-429 is involved in regulation of NF-kappaBactivity by targeting IKKbeta and suppresses oncogenic activity in cervical cancer cells. FEBS Lett 2017; 591: 118-128.

[31] Guo CM, Liu SQ and Sun MZ. miR-429 as biomarker for diagnosis, treatment and prognosis of cancers and its potential action mech-

anisms: a systematic literature review. Neoplasma 2019; 67: 215-228.

[32] Ye ZB, Ma G, Zhao YH, Xiao Y, Zhan Y, Jing C, Gao K, Liu ZH and Yu SJ. miR-429 inhibits migration and invasion of breast cancer cells in vitro. Int J Oncol 2015; 46: 531-538.

[33] Li D, Wang H, Song H, Xu H, Zhao B, Wu C, Hu J, Wu T, Xie D, Zhao J, Shen Q and Fang L. The microRNAs miR-200b-3p and miR-429-5p target the LIMK1/CFL1 pathway to inhibit growth and motility of breast cancer cells. Oncotarget 2017; 8: 85276-85289.

[34] Ramos AR, Elong Edimo W and Erneux C. Phosphoinositide 5-phosphatase activities control cell motility in glioblastoma: two phosphoinositides PI(4,5)P2 and PI(3,4)P2 are involved. Adv Biol Regul 2018; 67: 40-48.

[35] Ben-Chetrit N, Chetrit D, Russell R, Korner C, Mancini M, Abdul-Hai A, Itkin T, Carvalho S, Cohen-Dvashi H, Koestler WJ, Shukla K, Lindzen M, Kedmi M, Lauriola M, Shulman Z, Barr H, Seger D, Ferraro DA, Pareja F, Gil-Henn H, Lapidot T, Alon R, Milanezi F, Symons M, Ben-Hamo R, Efroni S, Schmitt F, Wiemann S, Caldas C, Ehrlich M and Yarden Y. Synaptojanin 2 is a druggable mediator of metastasis and the gene is overexpressed and amplified in breast cancer. Sci Signal 2015; 8: ra7.

Supplementary Table 1. qPCR primers and siRNA/miRNA sequence

| qPCR primers	for	Rew
GAPDH	GGTGGTCTCCTCTGACTTCAACA	GTTGCTGT AGCCAAA TTCGTTGT
LINC01234	GAATCAACTCTGCCAACAC	GCCTCATCTACATCTACTCTT
PACRGL	TTGCTACCTAGACTGATTCC	GACCAACAACGACACTTAG
C6orf25	CTGCGGAGGAGTCTCTCATC	AGAGTCCAGGGAGCGTAGG
CBFB	GCTCGGAAATCGCTTTTGTGG	CGGCTAGGTGTTTGTCGCT
CLIC1	CACCAACAAGATTGAGGAAT	CCTTCTCCAGATTGTCATTG
DCUN1D5	GCCTTGATATTGATACTGCTAA	CACCATCTTCATCATAGTTACTAA
PROM1	AATAAGCATTGGCATCTTCTAT	TTGTCCTTGGTAGTGTTGTA
SYNJ1	TTGATATGGAAGGTGATGTTG	TGAAGATGGCTGGAGATG
E2F3	AGTTGTGAAAGCCCCTCCAG	AGCCAAGTCTTTGGAAGCGG
NOG	TGGTGGACCTCATCGAACAC	ATGAAGCCTGGGTCGTAGTG
ROCK1	TTCGGATTGTTTGCTGGATGG	TGCACCTCTACCAATCACCTTC
SMAD2	ACAAGAAGGCATATAGGAAGA	ACTATCACTTAGGCACTCAG
TBL1XR1	TTATTTTGGGGGTGGTTGGAGG	CAGGATATAACCCATTGGCAGT
UBE2D1	CACTATTATGGGGCCTCCTG	AGTCAGAGCTGGTGACCATT
YWHAB	GAGAAGATAGAGGCAGAACT	CTGGTTGTGTAGCATTGG
hsa-U6	CTCGCTTCGGCAGCACA	AACGCTTCACGAATTTGCGT
hsa-miR-429	CCGCGCTAATACTGTCTGG	GTGCACGCTCCGAGGT
hsa-miR-3619	CCGCGCTCAGCAGG	GTGCACGCTCCGAGGT
hsa-miR-29a	CCGCGCTAGCACCATCT	GTGCACGCTCCGAGGT
hsa-miR-124	TCGCGCT AAGGCACG	GTGCACGCTCCGAGGT
hsa-miR-125b	TCGCGCTCCCTGAGAC	GTGCACGCTCCGAGGT
hsa-miR-143-3p	TCGCGCTGAGA TGAAGC	GTGCACGCTCCGAGGT
hsa-miR-196a	TCGCGCT AGGT AGTTTCA TGT	GTGCACGCTCCGAGGT
hsa-miR-204-5p	TCGCGCTTCCCTTTGT	GTGCACGCTCCGAGGT
hsa-miR-218	TCGCGCTTGTGCTTGAT	GTGCACGCTCCGAGGT
siRNA/miRNA sequence		
si-LINC01234	GGATTTGGATGTATGGGTT	
si-SYNJ1	GTCGGAACCTGGAATGTGA	
hsa-miR-429 mimic	sense: UAAUACUGUCUGGUAAAACCGU	
	antisense: ACGGUUUUACCAGACAGUAUUA	
has-miR-429 inhibitor	ACGGUUUUACCAGACAGUAUUA	
sh-LINC01234	GGATCCGGATTTGGATGTATGGGTTCTTCCTGTCAGAAACCCATACATCCAAATCCTTTTTGAATTC	

1
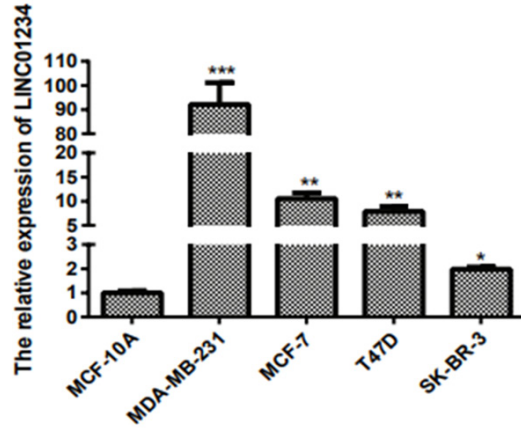
Supplementary Figure 1. LINC01234 is upregulated in TNBC. LINC01234 expression in different breast cancer cells. TNBC, Triple-Negative Breast Cancer. The data were representative of 3 independent experiments with the mean ± standard deviation. *$P<0.05$, **$P<0.01$, ***$P<0.001$.
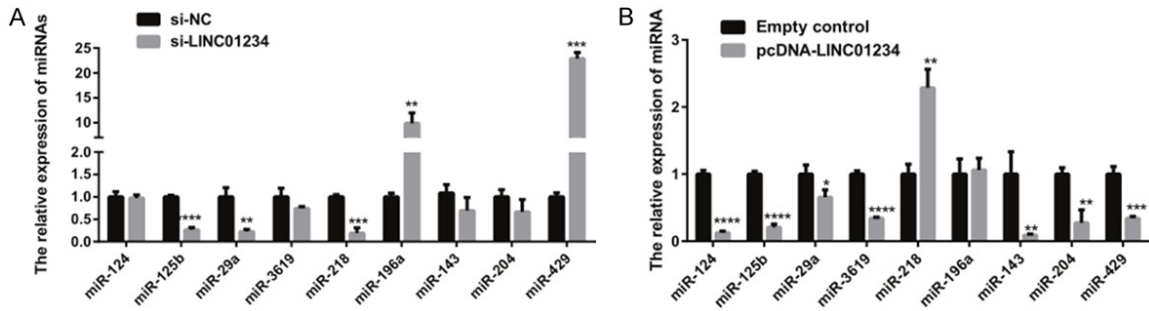
Supplementary Figure 2. qRT-PCR analysis of miRNAs expression in MDA-MB-231 cells transfected with si-LINC01234 (A) or pcDNA-LINC01234 (B). **$P<0.01$, ***$P<0.001$, ****$P<0.0001$.
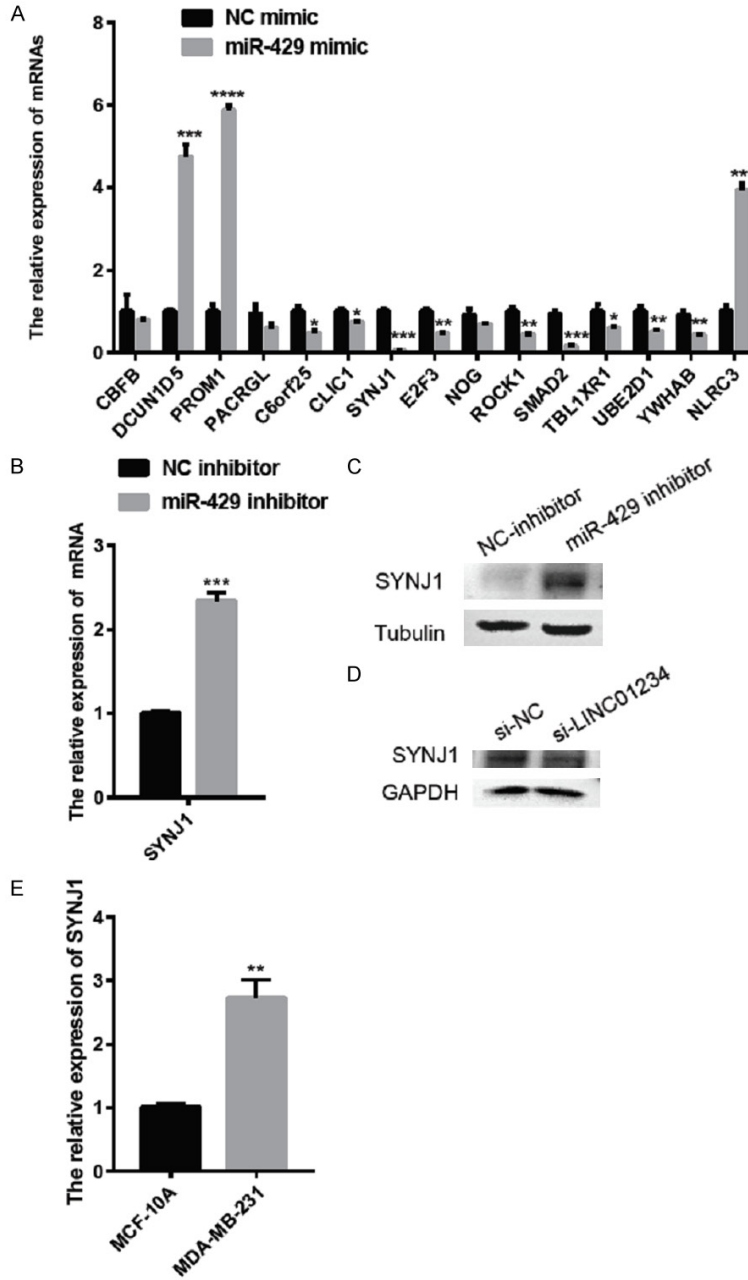
Supplementary Figure 3. A. qRT-PCR analysis of mRNA expression in MDA-MB-231 cells transfected with miR-429 mimic. B. qRT-PCR analysis of SYNJ1 expression in MDA-MB-231 cells transfected with miR-429 inhibitor. C. Western blot analysis of SYNJ1 expression in MDA-MB-231 cells transfected with miR-429 inhibitor. D. Western blot analysis of SYNJ1 expression in MDA-MB-231 cells transfected with si-LINC01234. E. The expression of SYNJ1 was significantly upregulated in MDA-MB-231 cells compared with MCF-10A. $^*P<0.05$, $^{**}P<0.01$, $^{***}P<0.001$, $^{****}P<0.0001$.